

Cell geometry effect on in-plane energy absorption of periodic honeycomb structures

F. N. Habib¹ · P. Iovenitti¹ · S. H. Masood¹ · M. Nikzad¹

Received: 3 June 2017 / Accepted: 29 August 2017 / Published online: 9 September 2017
© Springer-Verlag London Ltd. 2017

Abstract With advances in 3D printing technology, now honeycomb structures can be made with virtually unlimited unit cell geometries and cell arrangements giving a wide range of possible mechanical properties. However, studies on such structures have been mainly limited to the hexagonal honeycombs with little work done on other cell geometries. This paper investigates the effect of unit cell geometry on the in-plane compressive response and energy absorption behaviour of honeycombs using full-scale non-linear numerical simulations. Nine types of honeycombs are designed from different unit cell shapes, but having the same relative density. Finite element analysis is used to simulate the honeycombs' behaviour under uniaxial compression loading. The results showed that unit cell geometry and cell arrangement affect the honeycombs' compressive response significantly and provide different energy absorption characteristics. This comparison study shows that the honeycombs in which the deformation mode is dominated by bending of cell edges present a lower stiffness (effective modulus) and compressive strength, but a smoother plateau stress. The honeycombs having their deformation mode dominated by plastic buckling present a higher stiffness with less stable and undulated plateau stress. The results of this study provide more understanding in predicting the global behaviour of honeycomb structures and their energy absorption characteristic through their micro-topology. The effect of cell shape and its arrangement on the selection of honeycombs for energy absorption application is discussed and a

methodology is proposed to balance the energy absorption with maximum transmitted stress, which is crucial for energy-absorbing design of structures.

Keywords Cell geometry · In-plane compression · Finite element analysis · Stress-strain diagram · Energy absorption diagram · 3D printing

1 Introduction

Honeycomb is a two-dimensional prismatic cellular material with a regular and periodic microstructure. Owing to their lightweight and unique mechanical properties, polymeric and metallic honeycombs are widely used as cores for sandwich panel structures and energy absorbers.

The compression response and mechanical properties of honeycombs are not just a function of the base material properties and the relative density, but also a function of the local topological properties [1–3]. Impact response and deformation mechanism is vital in the design of honeycombs. They could be applied and used safely only after understanding the relation between their micro-topology and macro-dynamic responses, and predicting the honeycombs' performance through their local microstructures [4].

For energy absorption applications, cellular structures, including honeycombs, can absorb a large amount of energy without producing a high stress level on the protected object. However, designing and using honeycombs for energy absorption applications with limited stress threshold demands, in addition to the material selection, much attention in choosing the correct cell geometry, cell arrangement and design parameters. This is essential because the aim of using these energy-absorbing structures is not just to absorb a certain amount of energy produced from an impact, but also to keep

✉ F. N. Habib
fhabib@swin.edu.au

¹ Department of Mechanical and Product Design Engineering, Faculty of Science, Engineering and Technology, Swinburne University of Technology, Melbourne, VIC -3122, Australia

the transmitted force to the protected object below the force threshold that can cause damage [1].

Different manufacturing techniques are used to produce honeycomb structures including expansion, corrugation, extrusion, casting [1] and recently 3D printing processes [5–7]. The latter has overcome most of the limitations of conventional manufacturing approaches of honeycombs to a great extent [8]. Now honeycombs of any cell geometry, different cell sizes and a wide range of material options including polymers, metals and ceramics are possible by 3D printing.

For impact energy absorption application, which is the focus of this paper, honeycombs can be used in the out-of-plane or in-plane directions. However, they can provide a more stable, smoother and constant plateau stress in the in-plane direction than out-of-plane [7], but less in magnitude [1].

Extensive research have been undertaken in the past to study the compressive behaviour of honeycombs, mostly of hexagonal cells, in both out-of-plane and in-plane directions. Regarding the in-plane loading, which is considered in this study, Papka and Kyriakides [9, 10] investigated compressive response of metallic hexagonal honeycombs experimentally and numerically when loaded in the in-plane direction. Ruan et al. [11] studied the in-plane dynamic crushing of hexagonal aluminium honeycombs using finite element analysis method. Mozafari et al. [12] studied the effect of foam-filling on energy absorption of aluminium hexagonal honeycombs. Bates et al. [5, 13] have experimentally investigated the in-plane compressive response and energy absorption of regular and density gradient elastomeric hexagonal honeycombs under quasi-static loading. Hedayati et al. [7] studied the in-plane compressive properties of additively manufactured thick polymeric hexagonal honeycombs using analytical, numerical and experimental methods and derived analytical equations for the elastic properties of these honeycomb structures. Habib et al. [12] studied the in-plane compressive response and energy absorption capacity of 3D printed polymeric hexagonal honeycombs using experimental and numerical methods.

Some other studies have investigated the mechanical properties of honeycombs of cell geometries other than hexagonal. Gibson and Ashby [1] derived the analytical equations for elastic properties of triangular and quadratic honeycombs based on unit cell analysis. Wang and McDowell [14] studied the in-plane mechanical properties of periodic metallic honeycomb structures of seven different building unit cell geometries. In that study, the effective elastic modulus and initial yield strength of the seven metallic honeycomb structures with relative densities of 0.1 to 0.3 are reported as functions of their relative densities. Hedayati et al. [8] investigated the in-plane elastic compressive response of additively manufactured polymeric octagonal honeycombs using numerical and experimental methods and derived analytical equations for elastic properties of these honeycomb structures. However, aforementioned studies were limited to honeycomb's behaviour in the

linear elastic region and did not study the honeycombs' behaviour beyond the elastic regime nor their energy absorption characteristics.

Papka and Kyriakides [15] studied the in-plane compressive response and crushing of a honeycomb of circular cells subjected to displacement controlled loading both experimentally and numerically. The honeycomb was made by bonding together polycarbonate extruded tubes in a hexagonal close packed arrangement. Their results showed that if the geometric and material properties of cellular materials are established and modelled appropriately, the compressive properties of such materials can be simulated with high accuracy.

Liu et al. [4] studied the effect of unit cell geometry and arrangement on the in-plane dynamic crushing of honeycombs of equilateral triangular and quadratic cells with regular and staggered arrangements using finite element analysis. The results showed that the honeycombs of various cell geometries and cell arrangements will display different crushing deformation behaviour and properties. The study also showed that the plateau stress increases with the impact velocity by a quadratic law. The authors formulated empirical equations for these honeycombs in terms of impact velocity, and the cell topology and geometrical parameters. Their work also was limited to study just two types of honeycombs (triangular and quadratic).

Despite the large body of work on honeycombs, there seems to be little research on the effect of cell shape on the in-plane compressive response and energy absorption capacity of honeycombs. This investigation fills this gap and provides an in-depth numerical study on the effect of cell shape and cell arrangement of a range of honeycombs on their compressive properties and crushing behaviour. The compressive response and energy absorption of honeycombs built with different unit cell geometries are studied using Abaqus/Explicit finite element analysis (FEA) package. The results are presented and compared, and the conclusions are made.

2 Materials and methods

The mechanical properties of cellular structures depend on the material properties of the cell walls, the cell topology and the relative density. In this study, in order to investigate the influence of cell topology and geometry on the compressive behaviour of honeycombs, the other two parameters (the base material type and the relative density) will be kept constant. Thus, nine honeycombs of different building unit cell geometries, or cell arrangements, are designed. All the honeycombs have a uniform cell wall thickness of 0.6 mm, the same number of cells in both the main in-plane directions (12×12 cells), but with different global dimensions. They were designed so as to have a constant relative density of 15%. Fig. 1 shows the computer-aided design (CAD) models of the nine honeycombs and Table 1 lists their topological structure (edge

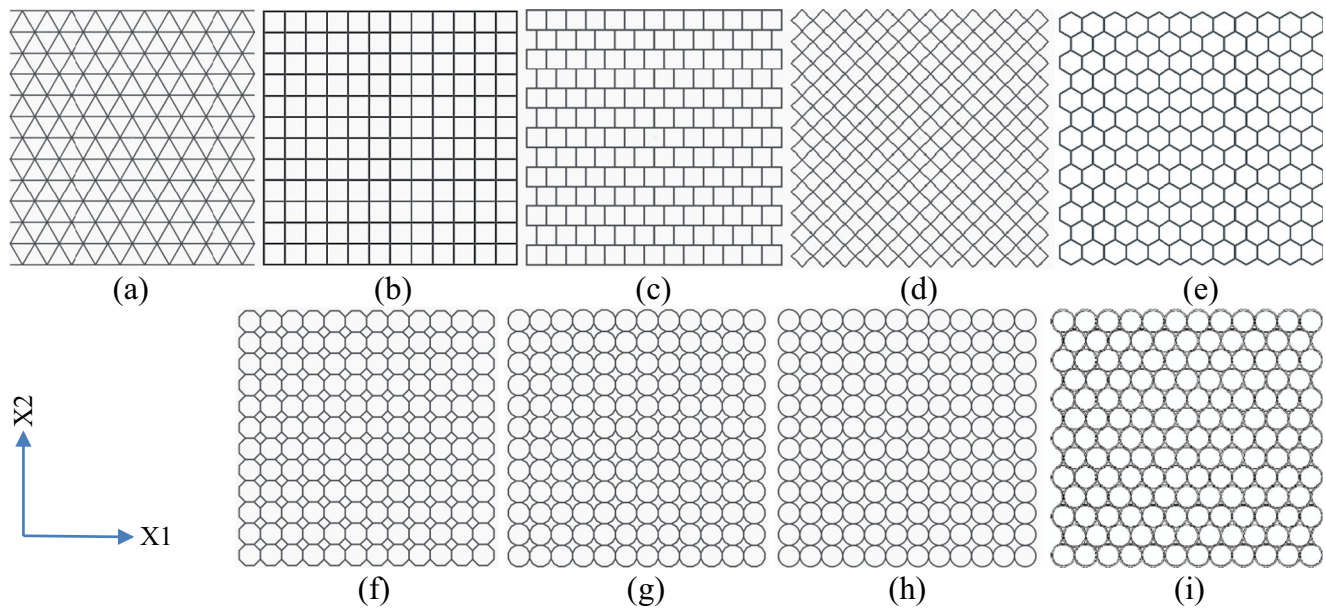


Fig. 1 The nine honeycomb types of different building unit cell geometry or cell arrangement; **a** triangular, **b** regular quadractic, **c** staggered quadractic, **d** diamond, **e** hexagonal, **f** octagonal, **g** dodecagonal, **h** regular circular, **i** staggered circular

connectivity; which is the number of edges that meet at a vertex) and dimensional parameters. In Fig. 1, the honeycomb (a) is built from equilateral triangles (internal angles = 60°) arranged in a hexagonal pattern with edge connectivity of 6. Honeycomb (b) is composed of quadratic (internal angles = 90°) cells with regular arrangement of cells and edge connectivity of 4, which becomes 3 in staggered arrangement of cells in honeycomb (c) by shifting the even rows to the right by half edge. Honeycomb (d) is made of diamond cells, which is the same as quadratic cells of regular arrangement honeycomb (b) in internal angles value and edge connectivity but the cells have been oriented by 45° . Honeycombs (e), (f), (g) and (h) are made of regular hexagons (internal angles = 120°), octagons (internal angles = 135°), dodecagons (internal angles = 150°) and circular cells with edge connectivity of 3, 3, 3 and 4, respectively. The honeycomb (i) also consists of circular cells with edge connectivity of 4 but is arranged staggered.

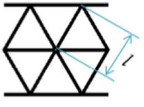
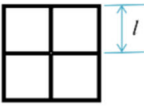
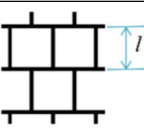
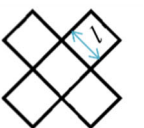
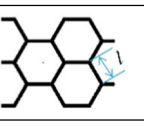
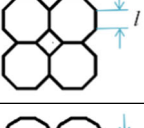
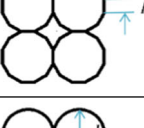
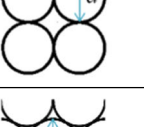
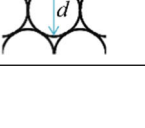
3 Finite element analysis of the honeycomb structures

The honeycombs material is assumed to be FDM Nylon12, and modelled as isotropic and elastic—perfectly plastic with mechanical properties adopted from our previous study [6] and listed in Table 2. In that experimental work, we calibrated our numerical technique against the mechanical tests and it has been shown that our numerical simulation approach and this simplified material model could reproduce experimental results with good agreement.

Abaqus/Explicit package [16] was employed to simulate the honeycombs' behaviour under low speed uniaxial compressive loading of 1 m/s. Shell elements of type S4R, 4-nod reduced integration, were used to model the honeycombs cell walls. Through convergence studies, it was found that the element size of 0.6 mm and five integration points through the thickness of the elements provide sufficiently accurate results with a reasonable computational time. To keep consistency, all the honeycombs structures were discretised in the same way. In the finite element (FE) model, honeycombs were compressed between two rigid plates as shown in Fig. 2a. To prevent the penetration of contacted surfaces, a general contact algorithm (Explicit) was defined for honeycomb cell walls' interaction with themselves and with the top and bottom plates during the crushing simulation. In order to decrease the model size and thus the computational time, the out-of-plane depth of FE model of all honeycombs was set to 1.2 mm (2 shell elements in depth), and to prevent the honeycombs' FE model from global buckling during the compression, all nodes of the honeycomb structures were constrained to translate in the out-of-plane direction, but they were free to move in both the main in-plane directions (X1 and X2 directions in Fig. 1). All degrees of freedom of the bottom plate were set to zero. The top plate was allowed to move just in the vertical direction as illustrated in Fig. 2b. The top plate compressed and crushed the honeycomb when moved downwards towards the bottom plate with a constant speed of 1 m/s.

When each honeycomb was crushed in X2 direction, the force and displacement data was obtained for 1000 evenly spaced time intervals during the loading as required by ISO 13314:2011 [17] to calculate the plateau stress and plateau

Table 1 Topological structure and dimensions for honeycombs of 15% relative density made from different regular (of equal polygon sides or diameter) shapes and uniform cell thickness of $t = 0.6$ mm

Unit cell label	Unit cell design and arrangement	Edge connectivity	Design parameter (mm)	Overall honeycomb structure dimensions	
				X1	X2
Triangular		6	$l=13.42$	161.64	140.06
Regular quadratic		4	$l=7.69$	92.88	92.88
Staggered quadratic		3	$l=7.69$	100.57	100.57
Diamond		4	$l=7.69$	131.35	131.35
Hexagonal		3	$l=4.44$	89.40	92.88
Octagonal		3	$l=3.93$	114.37	114.37
Dodecagonal		3	$l=2.73$	122.86	122.86
Regular circular		4	$d=10.75$	129.60	129.60
Staggered circular		4	$d=14.00$	168.60	160.10

end. For the hexagonal honeycomb structure, the simulation was performed in both X1 and X2 directions as it was found that its deformation mode in each direction is a good representative of other structures' deformation behaviour.

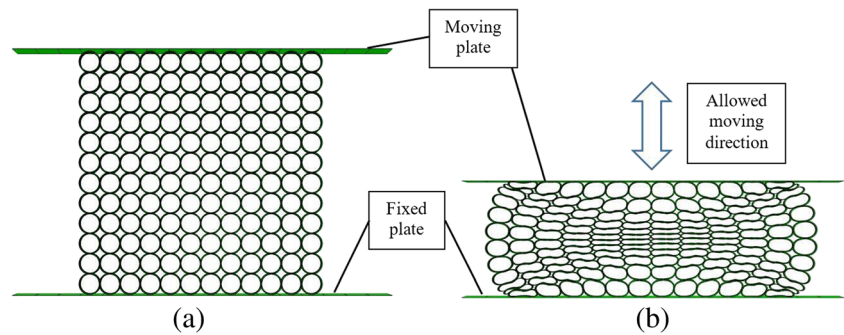
Table 2 Material properties of Nylon12 used in the FEA [6]

Material	Elastic modulus	Poisson's ratio	Density	Yield stress
Nylon12	1282 (MPa)	0.33	900 kg/m ³	32 (MPa)

4 Results and discussion

The cell collapse mechanism and stress-strain profile obtained from the numerical simulations of the studied honeycomb structures were found to be in good agreement with the experimental work available in literature. For example, the general stress-strain profile of our numerical study can be compared to the experimental work done on the regular quadratic honeycomb structure by Vesenjāk et al. [18], to the experimental work of our team on hexagonal honeycombs in both X1 and

Fig. 2 **a** FEA setup and boundary conditions. **b** The honeycomb compression by moving the top rigid plate towards the fixed bottom rigid plate



X2 directions [6], and to the experimental work on staggered circular honeycombs by Papka and Kyriakides [15].

4.1 Deformation mode

Under displacement controlled loading, the compressive response of a honeycomb structure is characterised by a relatively sharp rise to a stress maximum followed by an extended stress plateau which is ended by a sharp rise in stress. In the initial rising region, the deformation is elastic and basically uniform throughout the structure. Following the stress maximum, the structure yields and the deformation localises in a narrow zone of cells. This eventually causes the collapse of these cells until the contact between the cell walls stops their deformation and causes spreading of the deformation to other (usually the adjacent) cells where the same process is repeated. The process of propagation of the collapsed cells happens at a relatively constant stress level called plateau stress and continues until all the cells have collapsed and the structure densified. This causes a sharp rise of stress and the densified structure behaves like the solid material. It is worth mentioning that in real foams and honeycombs, the deformation is localised in the bands basically because of naturally occurring statistical variations in local cell dimensions and defects. Such defects and inconsistencies are unavoidable in natural and manufactured parts. However, in this paper, for the finite element study, the structures were assumed to be totally uniform and defect free.

Table 3 presents the deformation behaviour of the nine honeycomb structures at different stages obtained from the numerical simulations. Despite that all of the honeycomb structures having the same relative density, and the same base material, it can be observed that they behave differently under compressive loading due to the difference in the unit cell geometry, or cell arrangement. The deformation behaviour of the nine investigated structures can be broadly classified into two main categories:

Firstly, the honeycomb structures which show a “I” band deformation mode perpendicular to the loading direction. The collapse of cells in these structures is dominated by plastic buckling of cell edges row by row. This collapse mechanism

leads to undulating stress-strain curve with the collapse of each row (in some cases a pair of adjacent rows). This behaviour can be observed clearly in regular quadratic, staggered quadratic, hexagonal-X2 and staggered circular. Secondly, the structures which experience an inclined “I” band deformation show more stable plateau stress with less undulating behaviour. The deformation mode in these structures is dominated by bending of cell edges. This deformation behaviour and stable plateau stress is more apparent in the structures which develop double intersected inclined “I” band modes. In this case, the deformation mode is close to an “X” band, and this can be seen clearly in the honeycombs of diamond, hexagonal (in X1 direction) and regular circular cells.

However, some honeycomb structures show a deformation behaviour in between the two aforementioned deformation modes, such as octagonal and dodecagonal honeycombs. And the triangular honeycomb deformation mode is almost arbitrary.

4.2 Stress-strain diagram

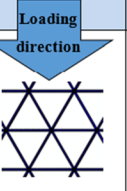
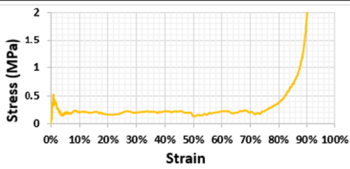
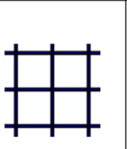
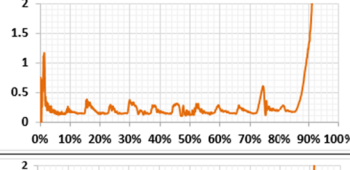
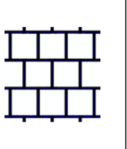
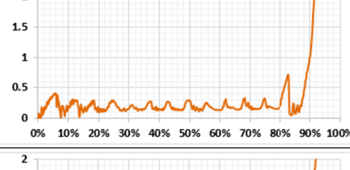

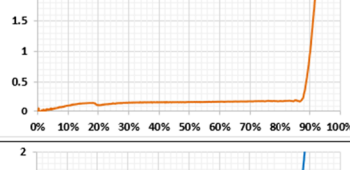
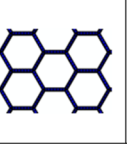
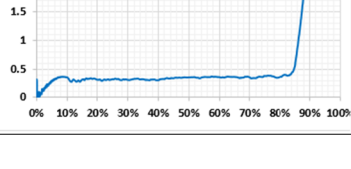

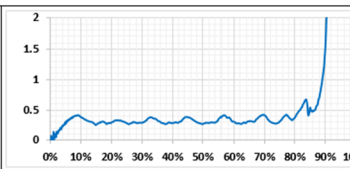
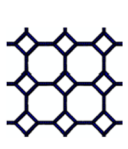
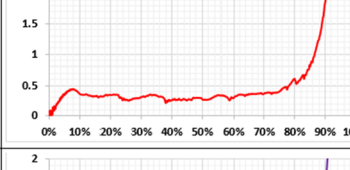
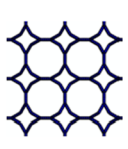
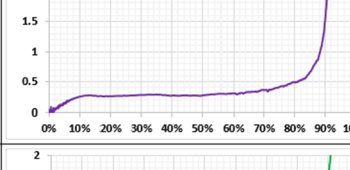
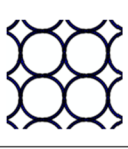
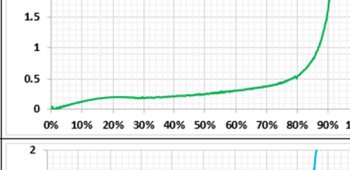
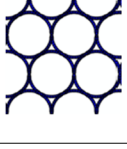
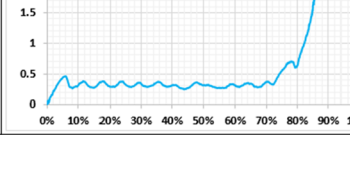
The force-displacement data obtained from FE analyses were converted to the compressive stress-strain data in accordance with ISO 13314:2011 [17]. The compressive load carried by the honeycomb structure at any given moment divided by original cross-sectional area perpendicular to the loading direction within the gage boundaries was referred to as the stress (σ) and expressed in force per unit area (MPa). The stress was plotted against the instantaneous overall displacement (δ) of the moving (top) plate during the compression simulation normalised by the original height (gauge length) of the honeycomb structure along the loading direction, and was called the compressive strain (ϵ). Table 4 shows the resulting compressive stress-strain diagrams of the honeycomb structures from the numerical simulations under a constant uniaxial compressive displacement loading of 1 m/s.

Regarding their compressive behaviour and stress-strain diagram, the structures can be classified into three categories. Firstly, the structures that show a high initial stiffness and peak stress. This group includes the honeycombs built from triangular and quadratic (regular arrangement) unit cells.

Table 3 Screen shots of deformation modes from numerical simulation of the honeycombs under constant uniaxial compressive displacement controlled loading of 1 m/s

Unit cell geometry	$\epsilon=0\%$	$\epsilon=20\%$	$\epsilon=40\%$	$\epsilon=60\%$	$\epsilon=80\%$
Triangular					
Regular quadratic					
Staggered quadratic					
Diamond					
Hexagonal-X1					
Hexagonal-X2					
Octagonal					
Dodecagonal					
Regular circular					
Staggered circular					

Table 4 Uniaxial compressive stress-strain diagram for the honeycomb structures under uniaxial displacement controlled loading of 1 m/s

Topology	Honeycomb unit cell	Stress-strain diagram
Triangular		
Regular quadratic		
Staggered quadratic		
Diamond		
Hexagonal-X1		
Hexagonal-X2		
Octagonal		
Dodecagonal		
Regular circular		
Staggered circular		

Triangular structures are known for their mechanical strength and stiffness due to the axial loading of the cell members under loading. As shown in Table 4, the triangular honeycomb presents a high initial stiffness and yielding stress. The regular quadratic honeycomb structure also shows high initial stiffness and much higher yielding stress than triangular honeycomb. After yielding the stress-strain profile of the quadratic honeycomb remains undulating with the buckling of each row of cell edges. As mentioned above, for many energy absorption applications, the aim is not just about being able to absorb a certain amount of impact energy, but also about not producing a high stress level while absorbing the impact energy (as in human protective devices and delicate objects packaging applications). Producing a stress level higher than the stress threshold of the protected object would be harmful. As these structures produce a high initial yielding stress (much higher than their plateau stress), which may damage the object to be protected, they are not desirable for these impact absorbing applications.

Secondly, structures with deformation modes that are dominated by the bending of cell edges show much less stiffness and a stable and smoother stress-strain curve as in diamond,

hexagonal-X1 and regular circular honeycombs as shown in Table 4.

Thirdly, the honeycomb structures that involve cell walls laid parallel to the loading direction experience plastic buckling (as the cell walls are thick, 0.6 mm, elastic buckling does not occur) causing undulation of stress in the plateau region. It can be observed from Fig. 3 that the increase of buckling members share against bending members in cell walls, from left (a) to right (e), will cause an increase in undulating behaviour (peak and valley range magnitude) of stress in the plateau region. This can be seen in the honeycombs of the circular cells with no buckling member, then dodecagonal cells with share of buckling members 2 out of the 12 members of a cell (or 2/12), octagonal cells (2/8), hexagonal cells in X2 direction (2/6) and quadratic cells of 2/4. The undulation of stress in the plateau region for honeycombs of quadratic cells, both for regular and staggered arrangement, is very evident and it can be seen that the number of peaks is equal to the number of cell rows, whose vertical walls buckle one by one and cause these peaks and valleys. If we look at the stress-strain diagram of these structures in the opposite order from right (e) to left (a), from honeycombs of quadratic cells of regular and staggered

Honeycomb unit cell

Stress in plateau region

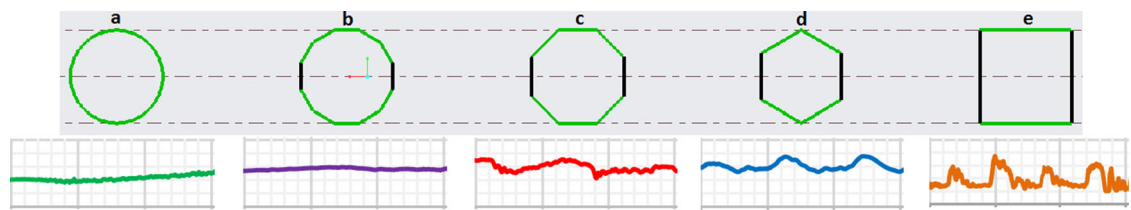


Fig. 3 Change in undulating behaviour of stress in plateau region due to the increase of buckling member's share of honeycombs' unit cells, coloured in black, from left honeycombs of regular arrangement of (a) circular, (b) dodecagonal, (c) octagonal, (d) hexagonal and (e) quadratic cells

arrangement to dodecagonal cells, it can be noticed that the plateau stress becomes increasingly smoother due to the same aforementioned reason, and the zigzag behaviour will totally disappear in honeycombs of regular circular (a) with no buckling members.

4.3 Plateau stress

The amount of energy absorbed in the initial elastic portion of the stress-strain diagram is relatively small. As most of the energy will be absorbed in the plateau region, the magnitude and length of the plateau stress, to a great extent, determines the energy absorption capacity of an energy absorber. The plateau stress of the honeycomb structures was calculated as the arithmetical mean of the stresses at 0.1% strain intervals between 20 and 40% compressive strain, and the plateau end was determined as a point on the stress-strain curve where the stress is 1.3 times the plateau stress, both in accordance with ISO 13314:2011 [17]. The plateau stress, and the magnitude of stress and strain at the plateau end are listed in Table 5. Regarding the plateau stress, it can be noted from Table 4 that the diamond and hexagonal (in X1 direction) honeycombs provide the most stable, long (high compressibility) and nearly constant plateau stress. However, its magnitude is much higher in the latter (more than twice), which means much more energy absorption.

4.4 Energy absorption and transmitted stress

For an energy absorber, the peak reaction force (maximum transmitted stress) would be kept below a threshold thus avoiding initial high peak stresses. Ideally, the reaction force (plateau force) should remain constant during the large deformation and the energy absorption process of the energy-absorbing structure. In this sense, the energy absorbers act as a kind of load-limiter, ideally possessing an approximate rectangular stress-strain characteristic [19].

Thus, the stress-strain profile of an ideal energy absorber is one that shows an infinite stiffness (vertical stress-strain diagram) in the elastic regime until a certain stress level, which should be kept below the damage threshold of the protected

object. Then, it deforms at a constant stress level in a horizontal line shape in the plateau regime until the plateau end strain, which is equal to the densification strain in this ideal case. After densification, the stress level rises sharply and the densified structure behaves like the solid material. However, this behaviour may not be achievable in reality. The closer the stress-strain diagram of an energy absorber is to this ideal profile, the better the energy absorber could be. Since the densification strain and onset strain of densification (plateau end strain) are different in reality [20], the optimum energy absorbers should be designed to absorb energy up to their plateau end strain, thus avoiding high stresses on the protected object.

The energy absorption (W) of a structure up to a strain, \mathcal{E} , is,

$$W = \int_0^{\mathcal{E}} \sigma(\mathcal{E}) d\mathcal{E} \quad (1)$$

which is simply the area under the stress-strain curve up to the strain \mathcal{E} .

The energy absorption diagram is a useful tool for engineering design and for developing the optimum energy-absorbing structure for a particular application. It builds a relationship between the amount of energy absorbed by the structure up to a stress, σ , as a function of the peak produced stress (maximum transmitted stress to the protected object). From the energy absorption diagram, one can understand whether an energy absorber is capable of absorbing the required impact energy within the tolerated stress limit. The absorbed energy per unit volume, given by the area under the stress-strain curve, was calculated for each honeycomb using Microsoft excel software.

The energy absorption diagrams for the studied honeycombs are presented in Table 6. The shoulder points in the energy absorption diagrams represent the optimum use of each structure, which corresponds to the end plateau (onset of densification) point in the stress-strain diagrams (Table 4) and the maximum efficiency point in the efficiency diagrams (Table 6). It can be seen that the hexagonal honeycomb provides the highest energy absorption of 0.273 J/cm^3 up to the end plateau when loaded in X1 direction while producing only

Table 5 Compressive properties of the studied honeycomb structures

Unit cell shape	Plateau stress, σ_{pl} (MPa)	Plateau end stress, σ_{ple} (MPa)	Plateau end strain, ϵ_{ple} (%)	Energy absorbed (W) up to the plateau end (J/cm^3)	Maximum produced stress up to the plateau end (MPa)	Efficiency at the plateau end (%)	Ideality at the plateau end (%)
Triangular	0.204	0.266	76.1	0.159	0.527	30	40
Regular quadratic	0.191	0.249	86.2	0.176	1.169	15	17
Staggered quadratic	0.178	0.231	87.1	0.171	0.719	24	27
Diamond	0.153	0.198	87.2	0.134	0.200	67	77
*Hexagonal-X1	0.314	0.408	83.7	0.273	0.408	67	80
Hexagonal-X2	0.304	0.395	80.3	0.248	0.418	59	74
Octagonal	0.302	0.393	74.6	0.233	0.443	53	71
Dodecagonal	0.283	0.368	71.4	0.195	0.376	52	73
Regular circular	0.199	0.259	51.5	0.091	0.264	34	67
Staggered circular	0.176	0.229	78.0	0.140	0.318	44	56

* The optimum honeycomb structure for energy absorption

0.408 MPa peak stress, as listed in Table 5 and illustrated in Fig. 4.

The efficiency parameter which is the ratio of energy absorbed (W) up to a stress, σ , to the maximum produced

Table 6 Energy absorption and efficiency diagrams of the honeycomb structures

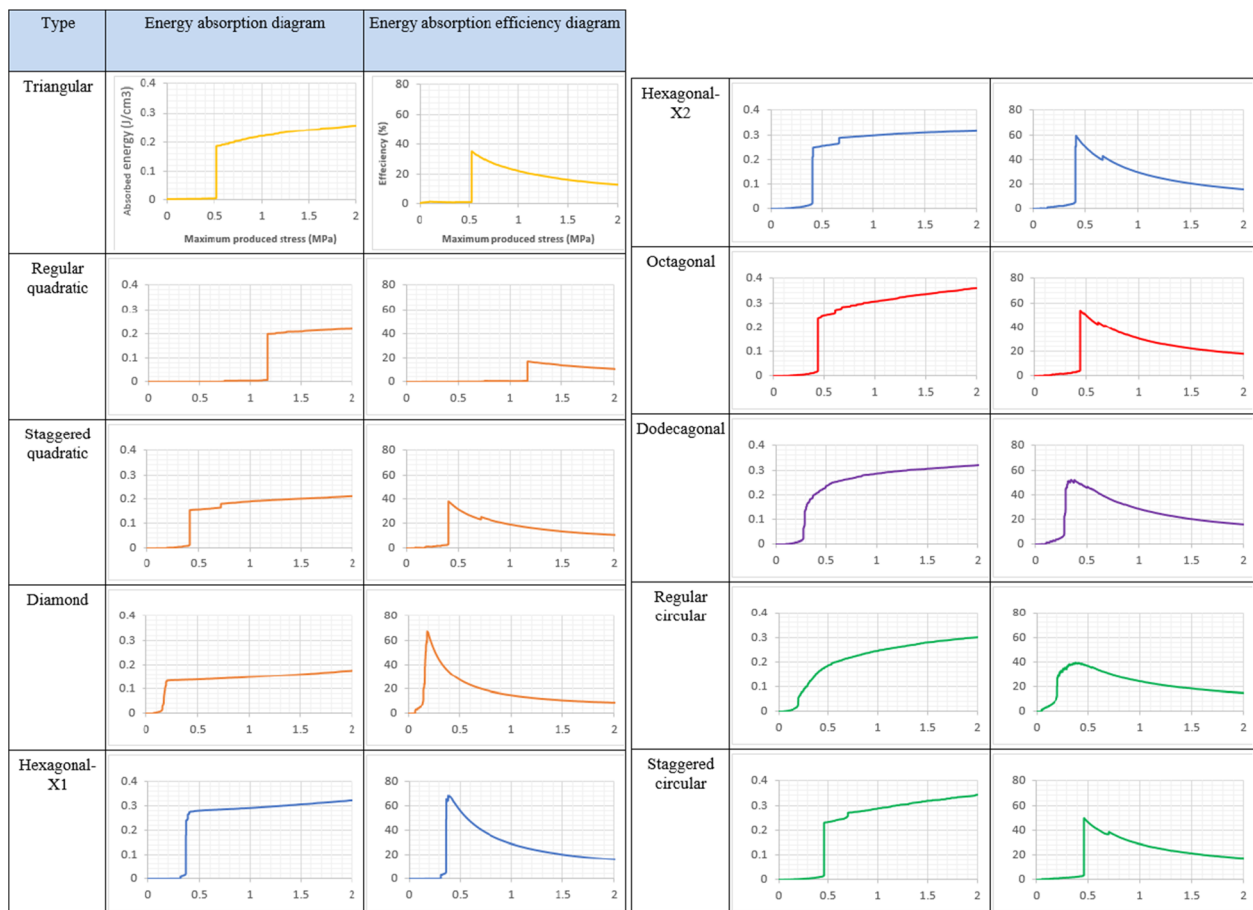
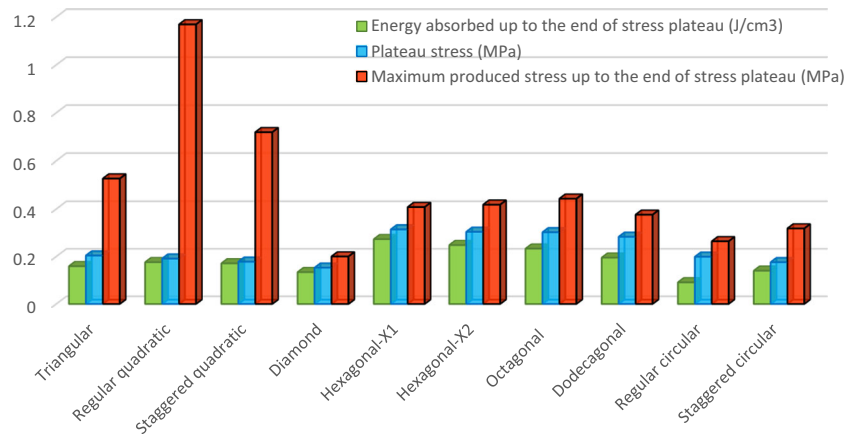


Fig. 4 Comparison of plateau stress, energy absorbed and maximum peak stress up to the plateau end for the studied honeycomb structures



stress [21] is also a useful tool to compare the studied structures.

$$E = \frac{\int_0^{\epsilon} \sigma(\epsilon) d\epsilon}{\sigma_{max}}, \tag{2}$$

Table 6 presents the efficiency diagrams of the studied structures. The maximum efficiency was achieved by dividing the energy absorbed up to the plateau end by the maximum produced stress up to that point, as listed in Table 5.

4.5 Ideality parameter

Ideality [21] is another parameter which compares the energy absorption capability of an energy absorber to an ideal energy absorber (of a rectangular stress-strain profile) when both are producing the same peak stress.

$$Ideality, I = \frac{\int_0^{\epsilon} \sigma(\epsilon) d\epsilon}{\epsilon \times \sigma_{max}}, \tag{3}$$

As shown in Eq. (3), ideality is also can be achieved by dividing the efficiency by the maximum strain experienced by the structure to absorb that amount of energy. The ideality

parameter at the plateau end is calculated for each topology and presented in Table 5. The efficiency and ideality parameter of the studied structures are also presented in Fig. 5.

To illustrate this point, Fig. 6 compares the energy absorption of the hexagonal honeycomb structure with that of an ideal structure up to its plateau end point ($\sigma_{ple} = 0.408$ MPa and, $\epsilon_{ple} = 83.7\%$ as listed in Table 5). It can be observed that the ratio of energy absorption of hexagonal honeycomb when loaded in X1 direction (area under its stress-strain curve) up to its plateau end to that of an ideal energy absorber with the same peak stress magnitude (area of the yellow shaded rectangle in Fig. 6) is 80%, which is also equal to the ideality parameter. The stress-strain profile of the hexagonal honeycomb in direction X1 provides a relatively high initial stiffness, then a relatively high and nearly constant and smooth plateau stress until a high strain level, and finally, the stress rises sharply, which is the closest to the ideal one compared to the other studied honeycombs. That is why it has the maximum energy absorption (0.273 J/cm³), the maximum efficiency (67%) and the maximum ideality (80%) with a relatively low maximum produced stress up to the end plateau (0.408 MPa). The hexagonal-X2 and octagonal honeycombs provide the next highest energy absorption capacity with

Fig. 5 Efficiency and ideality of the honeycomb structures at the plateau end

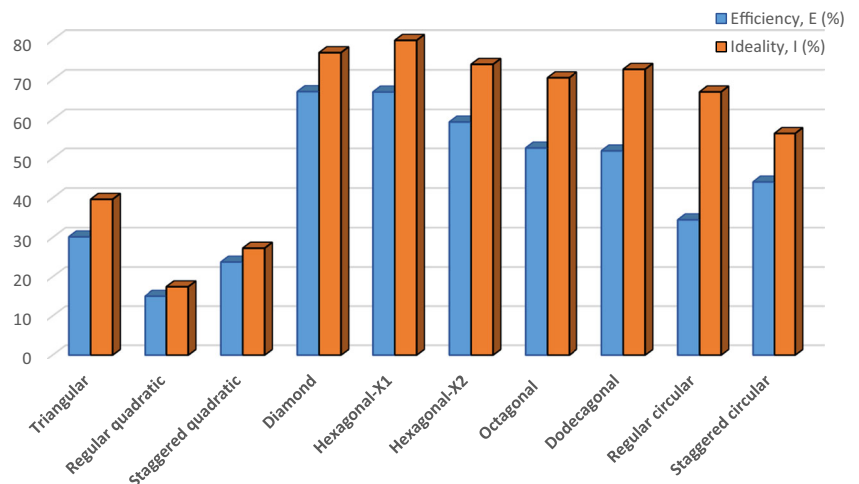
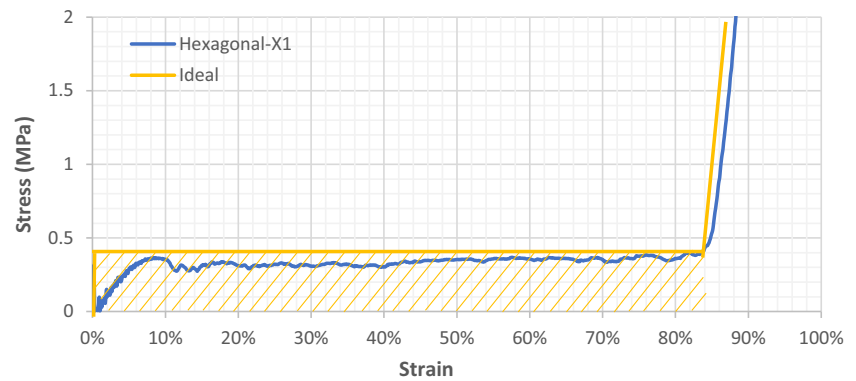


Fig. 6 The compressive stress-strain diagrams of the hexagonal honeycomb structure in the X1 direction compared to its counterpart ideal energy absorber



0.248 and 0.233 J/cm³, respectively, while producing higher stress levels (0.418 and 0.443 MPa, respectively) compared to the hexagonal-X1. Their efficiencies are 59 and 53% and ideality parameters are 74 and 71%, respectively. The diamond honeycomb provides a high efficiency (67%) and ideality (77%) due to its high compressibility (up to the strain 87.2%) and flat stress plateau. However, it absorbs low energy of 0.134 J/cm³ which is less than half of the energy absorbed by the hexagonal-X1.

The dodecagonal and circular (regular arrangement) honeycombs show a smooth stress-strain behaviour; however, they have less initial stiffness and the densification starts earlier (at 71.4 and 51.5% strains, respectively) and gradually. In these two structures (and also octagonal one for some extent), as all dodecagonal and circular cells collapse, higher stress levels are required to crush the small gaps between the cells, which leads to a gradual rise in stress, and this is not desirable for energy absorption applications. The triangular and quadratic honeycombs are also not desirable due to their high initial peak stresses.

5 Conclusion

The aim of this study was to investigate the effect of cell geometry and cell arrangement of geometrically different honeycombs on the compressive stress-strain behaviour and energy absorption characteristics. The CAD model of nine honeycombs of different unit cell geometry or cell arrangement, but with same relative density, was considered. Abaqus/Explicit code was used to simulate the compressive response of these honeycomb structures under displacement loading. The stress-strain curves obtained from the numerical analysis were analysed further by using energy absorption and efficiency diagrams and ideality parameter. The results showed that the cell geometry and cell arrangement affect the compressive stress-strain behaviour and energy absorption capacity of these structures significantly. Among the nine types of honeycomb structures that were analysed, the hexagonal honeycomb (in one of its main in-plane directions namely X1)

provided the best energy absorption behaviour and was the closest to the ideal energy absorber's behaviour with 80% ideality. It provides a relatively high initial stiffness, and a high, nearly constant, smooth and long plateau stress (up to 83.7% strain). The hexagonal honeycomb in X2 direction and octagonal honeycomb offer the next higher energy absorption but producing a less stable plateau stress and a higher transmitted peak stress. This is due to some vertical walls of these two structures lying in the loading direction which deform by plastic buckling and cause undulating deformation behaviour. As the ratio of buckling members to bending members increases, the buckling deformation and undulating effect of stress-strain diagram in the plateau region dominate even further, as it was found in the quadratic honeycombs of both regular and staggered arrangement. In the staggered circular honeycomb, at some stage of deformation, its cells shape becomes close to the staggered quadratic honeycomb cells, so to some extent, it experiences the same undulating and instability behaviour. Dodecagon and circular honeycombs, with bending dominated behaviour, show smoother stress-strain behaviour with low initial stiffness and gradual increase in plateau stress. The main disadvantage of triangular and regular quadratic honeycombs for energy absorption applications is their high initial peak stress, which is much higher than their plateau stress. The results of this comparative finite element study provide more insight into the effect of microstructure on the macro-dynamic response of honeycombs of different cell geometry, which is crucial for safe use of honeycombs for different engineering applications.

References

1. Gibson LJ, Ashby MF (1997) Cellular solids: structure and properties, second edn. Cambridge University Press, Cambridge, pp 1–510
2. Ashby MF (2006) The properties of foams and lattices. *Philos Trans R Soc A Math Phys Eng Sci* 364(1838):15–30
3. Srivastava V, Srivastava R (2014) On the polymeric foams: modeling and properties. *J Mater Sci* 49(7):2681–2692

4. Liu Y, Zhang X-C (2009) The influence of cell micro-topology on the in-plane dynamic crushing of honeycombs. *Int J Impact Eng* 36(1):98–109
5. Bates SRG, Farrow IR, Trask RS (2016) 3D printed polyurethane honeycombs for repeated tailored energy absorption. *Mater Des* 112:172–183
6. Habib FN et al (2017) In-plane energy absorption evaluation of 3D printed polymeric honeycombs. *Virtual Phys Prototyp* 12(2):117–131
7. Hedayati R et al (2016) Mechanical properties of additively manufactured thick honeycombs. *Materials* 9(8):613–636
8. Hedayati R et al (2016) Mechanical properties of additively manufactured octagonal honeycombs. *Mater Sci Eng C* 69:1307–1317
9. Papka SD, Kyriakides S (1994) In-plane compressive response and crushing of honeycomb. *J Mech Phys Solids* 42(10):1499–1532
10. Papka SD, Kyriakides S (1998) Experiments and full-scale numerical simulations of in-plane crushing of a honeycomb. *Acta Mater* 46(8):2765–2776
11. Ruan D et al (2003) In-plane dynamic crushing of honeycombs—a finite element study. *Int J Impact Eng* 28(2):161–182
12. Mozafari H et al (2015) In plane compressive response and crushing of foam filled aluminum honeycombs. *J Compos Mater* 49(26):3215–3228
13. Bates SRG, Farrow IR, Trask RS (2016) 3D printed elastic honeycombs with graded density for tailorable energy absorption. In: Park G (ed) *Active and Passive Smart Structures and Integrated Systems Proc SPIE Vol. 9799*, Las Vegas, United States
14. Wang A-J, McDowell D (2004) In-plane stiffness and yield strength of periodic metal honeycombs. *J Eng Mater Technol* 126(2):137–156
15. Papka SD, Kyriakides S (1998) In-plane crushing of a polycarbonate honeycomb. *Int J Solids Struct* 35(3):239–267
16. SYSTEMES D, Simulia, ABAQUS/CAE User's Manual (2014) ABAQUS Documentation V6 7
17. Standard, I., ISO 13314: 2011 (E) (2011) Mechanical testing of metals—ductility testing—compression test for porous and cellular metals. Ref Number ISO 13314(13314):1–7
18. Vesenjak M et al (2010) Cell shape effect evaluation of polyamide cellular structures. *Polym Test* 29(8):991–994
19. Lu G, Yu T (2003) In: Yu TX (ed) *Energy absorption of structures and materials*. Woodhead, Cambridge
20. Li QM, Magkiriadis I, Harrigan JJ (2006) Compressive strain at the onset of densification of cellular solids. *J Cell Plast* 42(5):371–392
21. Avalle M, Belingardi G, Montanini R (2001) Characterization of polymeric structural foams under compressive impact loading by means of energy-absorption diagram. *Int J Impact Eng* 25(5):455–472